*Smart Structures and Systems, Vol. 6, No. 8 (2010) 953-974*
DOI: http://dx.doi.org/10.12989/sss.2010.6.8.953


# Seismic response control of benchmark highway bridge using variable dampers

S.N. Madhekar[a] and R.S. Jangid*[b]

*Department of Civil Engineering, Indian Institute of Technology Bombay, Powai, Mumbai - 400 076, India*
*(Received April 17, 2009, Accepted April 16, 2010)*

**Abstract.** The performance of variable dampers for seismic protection of the benchmark highway bridge (phase I) under six real earthquake ground motions is presented. A simplified lumped mass finite-element model of the 91/5 highway bridge in Southern California is used for the investigation. A variable damper, developed from magnetorheological (MR) damper is used as a semi-active control device and its effectiveness with friction force schemes is investigated. A velocity-dependent damping model of variable damper is used. The effects of friction damping of the variable damper on the seismic response of the bridge are examined by taking different values of friction force, step-coefficient and transitional velocity of the damper. The seismic responses with variable dampers are compared with the corresponding uncontrolled case, and controlled by alternate sample control strategies. The results of investigation clearly indicate that the base shear, base moment and mid-span displacement are substantially reduced. In particular, the reduction in the bearing displacement is quite significant. The friction and the two-step friction force schemes of variable damper are found to be quite effective in reducing the peak response quantities of the bridge to a level similar to or better than that of the sample passive, semi-active and active controllers.

**Keywords:** benchmark highway bridge; MR damper; variable damper; friction force scheme; two-step friction force scheme.

## 1. Introduction

Highway bridges are lifeline structures and reduction of seismic vibration response is vital from the point of view of their serviceability. Due to lack of structural redundancy, bridges receive severe damage and generally lead to catastrophic failures during strong earthquakes. Northridge (January 17, 1994) and Kobe (January 17, 1995) earthquakes have demonstrated the importance of maintaining post-earthquake operation of bridges. Extensive damage to highway and railway bridges occurred in the Kobe earthquake, including the 18-span bridge at Fukae, Hanshin Expressways. Near-field ground accelerations with long pulses, one of the strongest ever recorded at the period ranging from 0.8 to 1.5 sec induced the damage. The failure of bridges in the Northridge earthquake was primarily due to large deck and bearing displacements. In highway bridges, damage of piers occurred from premature shear failure at the mid-height. Hence, for past several years, the research is focused on finding out more rational and substantiated solutions for protection of bridges from severe earthquake attack.

*Corresponding Author, Professor, E-mail: rsjangid@civil.iitb.ac.in
[a]Research Scholar
[b]Professor

Rigid connections between the deck and the substructure will reduce the deck displacement but increase the pier base shear. A wide variety of passive energy dissipation devices has been studied and implemented in the bridges worldwide to mitigate the seismic response (Kunde and Jangid 2003). Seismic isolation, though effective in reducing the mid-span deck accelerations, may result in increased mid-span and isolator displacements. Additional supplemental damping devices help in reducing the displacement of deck and pier base shear. To compare the performance and effectiveness of various control systems in protecting bridges from earthquakes, a benchmark problem on highway bridge has been recently developed by Agrawal *et al.* (2009). The problem consists of two phases; in phase I, the bridge deck is fixed to the outriggers; and in phase II, the bridge deck is isolated from the outriggers.

Kawashima and Unjoh (1994) used a displacement-dependent damping model of a variable fluid damper. Analytical results and shake table tests of a 30m long bridge indicated that there was significant reduction in deck displacement and deck acceleration. Spencer *et al.* (1997) demonstrated that MR fluid dampers can be controlled with small power supplies and the dynamic range of damping force level is quite large. Due to high energy dissipation capacity, MR dampers were considered appropriate for developing variable dampers. Variable dampers using viscous damper and MR damper, with a preset algorithm of damping force have been developed (Kawashima and Unjoh 1994, Ruangrassamee and Kawashima 2001, 2003, Ruangrassamee *et al.* 2004). The simulation results for a five-span continuous bridge have demonstrated their superior performance compared to passive dampers. Variable dampers have also been proved to be effective in reducing the response of a benchmark cable-stayed bridge (Ruangrassamee and Kawashima 2006). Tan and Agrawal (2009) presented sample passive, semi-active and active control system designs for the seismically excited benchmark highway bridge. Choi *et al*. (2006) developed a smart passive system, consisting of MR damper and an electromagnetic induction (EMI) system. The results of the numerical simulations show that the control system is beneficial in reducing seismic response of the benchmark highway bridge. The performance of fuzzy logic control systems for the earthquake protection of the bridge is also investigated (Reigles and Symans 2006, Ali and Ramaswamy 2006). In the past studies there has not been any attempt to investigate the effectiveness of variable dampers for the benchmark highway bridge.

In the present study, the performance of variable dampers for the earthquake protection of the benchmark highway bridge under real earthquake ground motions is investigated. The study puts forth simplified use of MR dampers as variable dampers. The specific objectives of the present study related to the earthquake response control of the benchmark highway bridge, are summarized as: (i) to investigate the performance of variable dampers by modeling the damping force with friction and two-step friction force schemes; (ii) to identify important parameters of the two-step friction force scheme affecting the response of the bridge; and (iii) to make a systematic comparison of response of variable dampers with the sample control strategies, provided in the problem definition.

## 2. The benchmark highway bridge model

The bridge model used for this benchmark study is that of the 91/5 overcrossing in Southern California, located very close to two major faults. A detailed description of the bridge can be found in Agrawal *et al.* (2009). The superstructure of the bridge consists of a two-span continuous pre-

stressed concrete (PC) box-girder and the substructure is in the form of PC outriggers. Each span of the bridge is 58.5 m long, spanning a four-lane highway, with two skewed abutments. The deck is supported by a 31.4 m long and 6.9 m high PC outrigger, resting on pile foundation. The total mass of the benchmark highway bridge is 4,237,544 kg and the mass of the deck is 3,278,404 kg. In the actual bridge, four conventional elastomeric bearings are provided at each abutment and four passive fluid dampers are installed between each abutment and the deck-end. In the evaluation model, lead rubber bearings (LRBs) are used in place of the elastomeric bearings. The uncontrolled response of the bridge is defined as the response of bridge, isolated with four LRBs at each deck-end. A 3D nonlinear finite element model of the bridge with 430 degrees-of-freedom ($N$) has been developed in ABAQUS, which is representative of the actual bridge. A simplified lumped mass finite element model considered for seismic investigations is shown in Fig. 1(a). Transverse (referred as $x$ direction) is the North-South and the longitudinal (referred as $y$ direction) is the East-West. For the purpose of analysis, the model is divided into 108 nodes.

The bridge superstructure is represented by 3D beam elements and modelled by B31 element in ABAQUS. Abutments and deck-ends are modelled by rigid links. The effects of soil-structure interaction at the abutments and approach embankments are also considered (Zhang and Makris 2002). Rigid links are used to connect the control devices between the deck-end and abutments. Each column of the bent is modelled by B31 element as stiff column cap, elastic column segments and nonlinear column segments. The bearings are modelled as shear element, by taking the vertical axial stiffness as infinite, and their torsional rigidity and bending stiffness are assumed to be zero. The bearings are idealized by bi-directional bilinear plasticity model (Zhang and Makris 2002). The pre-yield shear stiffness of bearings ($k_{b1}$) is 4800 kN/m and the post-yield shear stiffness ($k_{b2}$) is 600 kN/m. The yield displacement of bearing is 0.015 m and the yield force of the lead core versus weight of the deck ($Q_d$ / W) ratio is 0.05.

## 3. Modeling of damper control force

Friction dampers are used as passive control devices for a large number of structures. A properly designed friction damper provides a constant level of damping force over an entire stroke, resulting in a large amount of energy dissipation and the relative displacement can be effectively controlled. However, the sudden change of force creates larger acceleration in a structure, which can be limited, by using semi-active control strategy. In variable dampers, the damping force can be preset as a function of the stroke or velocity of the damper. Larger energy dissipation can be achieved by designing control schemes, thus reducing the relative movement between the deck and abutments. Friction force and two-step friction force damping schemes are proposed for variable dampers, in dynamic response analyses of the benchmark cable-stayed bridge (Ruangrassamee and Kawashima 2002). In the present study, the effectiveness of variable dampers with these schemes is investigated for the benchmark highway bridge. Fig. 1(b) shows the schematic diagram of a variable damper.

### *3.1 Variable damper with friction force scheme*

Conventionally the friction type damping force is generated by slippage between two materials under a normal force. Because of non-uniform roughness of contact surfaces, it is difficult to obtain smooth friction force. Also, the friction force that can be developed by a friction damper has

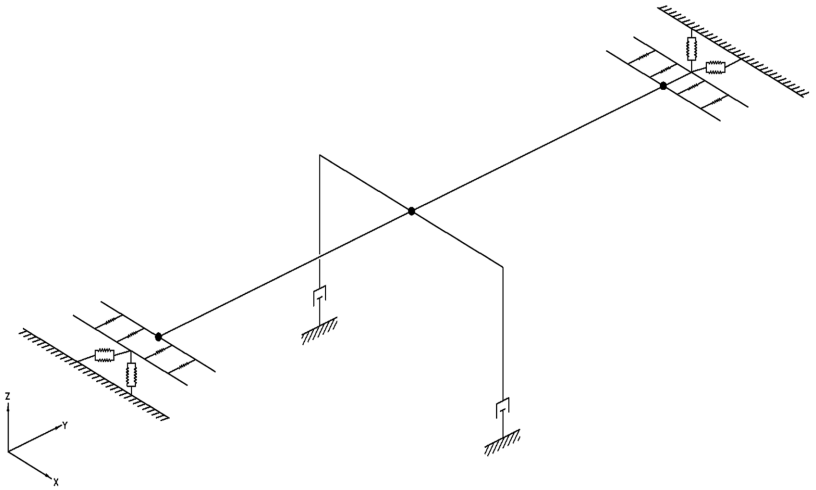


(a) 3D finite element model of the benchmark highway bridge

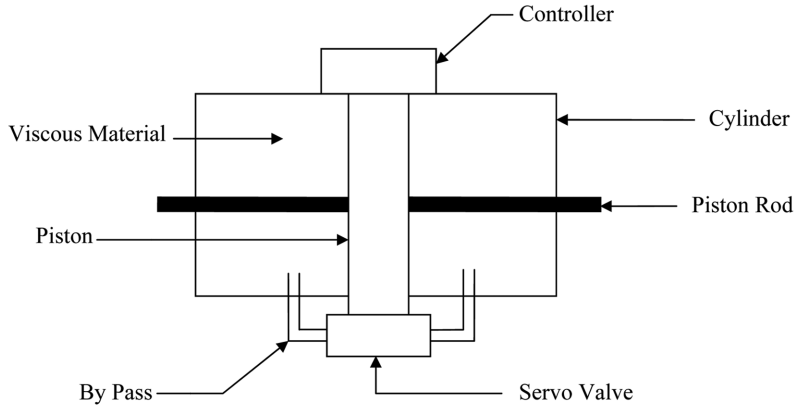


(b) Schematic of variable damper

Fig. 1 3D finite element model of benchmark highway bridge and schematic diagram of variable damper

limitations, as it depends on the coefficient of friction. To overcome such problems, variable dampers are used to generate the friction type damping forces. The response of a bridge can be effectively reduced by providing a constant restoring damping force, $F_D$ close to the force capacity of the damper. The force changes every time, when the velocity of the damper $\dot{u}$ changes its sign.

$$F_D = \begin{cases} F_F \ldots \dot{u} > 0 \\ -F_F \ldots \dot{u} < 0 \end{cases} \tag{1}$$

For the present study, the friction force $F_F$ is set equal to 1000 kN, the force capacity of MR dampers used in the design of sample semi-active controllers. Fig. 2(a) shows the mathematical model, force-displacement loop and force-velocity variation of friction force scheme of variable damper.

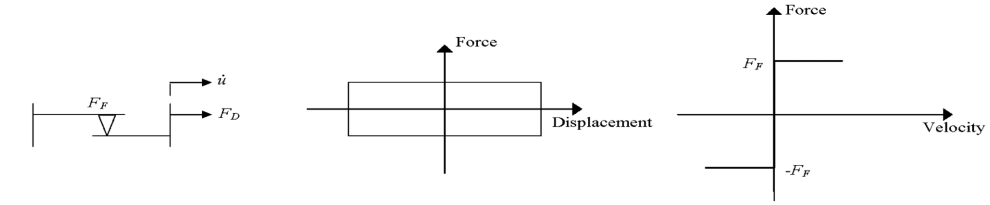


(i) Mathematical model (ii) Force-displacement (iii) Force-velocity

(a) Friction force scheme

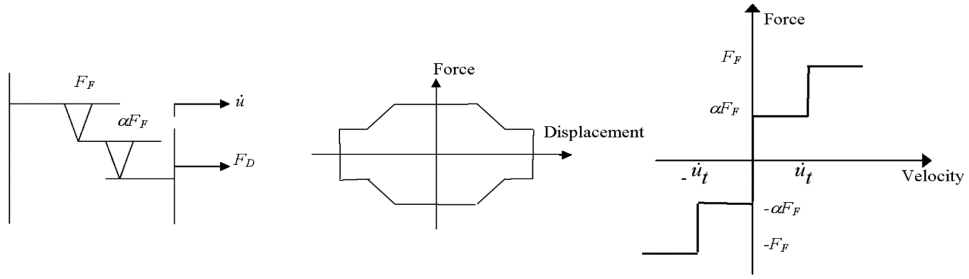


(i) Mathematical model (ii) Force-displacement (iii) Force-velocity

(b) Two-step friction force scheme

Fig. 2 Mathematical model, force-displacement loop and force-velocity relationship of friction and two-step friction schemes of variable dampers

### *3.2 Variable damper with two-step friction force scheme*

If the damping force level of a friction damper is large, it may decrease the energy dissipation, as the large damping force tends to lock the movement between the deck and abutments or piers. Further, it transfers larger inertial force from superstructure to substructure. A constant damping force, provided for the entire range of the stroke, increases the energy dissipation, resulting in a large reduction of response. Two-step friction force scheme modifies the characteristics of the friction force scheme. The damping force is preset as a function of velocity of the damper and is controlled in two steps.

$$F_D = \begin{cases} F_F \ldots \dot{u} > \dot{u}_t \\ \alpha F_F \ldots 0 < \dot{u} \le \dot{u}_t \\ -\alpha F_F \ldots -\dot{u}_t \le \dot{u} < 0 \\ -F_F \ldots \dot{u} < -\dot{u}_t \end{cases} \tag{2}$$

where $F_D$ is the damping force, $\dot{u}$ is the relative velocity between the deck and piers or deck and abutments, $F_F$ is the friction force produced by the damper, $\alpha$ is the coefficient, to represent the intensity of friction force at the 2nd step and $\dot{u}_t$ is the transitional velocity of the damper. Coefficient $\alpha$ ranges between 0 and 1. The smaller force $\alpha F_F$ functions to facilitate the movement of the damper when the piston is moving with a small velocity. Selection of the parameters $\alpha$ and $\dot{u}_t$ governs the response of the bridge. The dominant feature of the scheme is its simplicity in modelling. Fig. 2(b)

shows the mathematical model, force-displacement loop and force-velocity variation of the two-step friction force scheme of variable damper. For the present study, the benchmark highway bridge package is modified by incorporating SIMULINK models for variable dampers.

## 4. Governing equations of motion

A nonlinear response-history analysis in time domain is employed. The nonlinear finite element model of the bridge is considered excited under two horizontal components of earthquake ground motion, applied simultaneously along the two orthogonal directions. The responses in both directions are considered to be uncoupled and there is no interaction of forces. The equations of motion of the evaluation model are expressed in the following matrix form

$$[M]\{\ddot{u}(t)\} + [C]\{\dot{u}(t)\} + [K(t)]\{u(t)\} = -[M]\{\eta\}\{\ddot{u}_g(t)\} + [b]\{F(t)\} \tag{3}$$

$$\{u(t)\} = \{x_1, x_2, x_3, \ldots\ldots, x_N, y_1, y_2, y_3, \ldots\ldots, y_N\}^T \tag{4}$$

$$\{\ddot{u}_g\} = \begin{Bmatrix} \ddot{x}_g \\ \ddot{y}_g \end{Bmatrix} \tag{5}$$

where $[M]$, $[C]$ and $[K(t)]$ are the mass, damping and stiffness matrix, respectively of the bridge structure of the order $2N \times 2N$; $\{\ddot{u}(t)\}, \{\dot{u}(t)\}$ and $\{u(t)\}$ are structural acceleration, structural velocity and structural displacement vectors, respectively of size $N \times 1$; $\{\ddot{u}_g(t)\}$ is the vector of earthquake ground accelerations acting in two horizontal directions; $\ddot{x}_g$ and $\ddot{y}_g$ represent the earthquake ground accelerations in the transverse and longitudinal directions, respectively; $x_i$ and $y_i$ denote displacements of the $i^{th}$ node of the bridge in transverse and longitudinal directions, respectively; $\{F(t)\}$ is the control force vector; $\{\eta\}$ is the loading vector for the ground acceleration; and $\{b\}$ is the loading vector for the control forces.

The lumped mass matrix $[M]$ has a diagonal form. The stiffness matrix $[K(t)]$ is the combination of $[K_L + K_N(t)]$ where the $K_L$ is the linear part and $K_N(t)$ is the nonlinear part. The global damping matrix $[C]$ is expressed as a combination of the distributed inherent damping in the structure and soil radiation damping. The damping of LRBs is neglected. It is assumed that the properties of the system remain constant during the time-step of analysis. A MATLAB based nonlinear structural analysis tool has been developed, written as S-function. It is incorporated into the SIMULINK model of the benchmark highway bridge. The S-function solves the governing equations of motion using Newmark's step-by-step technique. For the present study, the time interval selected is 0.002 s.

## 5. Numerical study

The seismic response of the benchmark highway bridge is investigated for the six specified real earthquake ground excitations, namely (i) North Palm Springs (1986), (ii) TUC084 component of Chi-Chi earthquake, Taiwan (1999), (iii) El Centro component of 1940 Imperial Valley earthquake, (iv) Rinaldi component of Northridge (1994) earthquake, (v) Bolu component of Duzce, Turkey

Table 1 Peak ground accelerations of the six selected earthquake ground motions

| Earthquake | Type | PGA (g) EW | PGA(g) NS | Peak velocity EW (m/sec) | Peak velocity NS (m/sec) |
|---|---|---|---|---|---|
| North Palm Springs (1986) | Far field | 0.492 | 0.612 | 0.733 | 0.338 |
| Chichi (1999) | Near fault | 1.157 | 0.417 | 1.147 | 0.456 |
| Elcentro (1940) | Far field | 0.313 | 0.215 | 0.298 | 0.302 |
| Northridge (1994) | Near fault | 0.838 | 0.472 | 1.661 | 0.73 |
| Turkey (1999) | Near fault | 0.728 | 0.822 | 0.564 | 0.621 |
| Kobe (1995) | Near fault | 0.509 | 0.503 | 0.373 | 0.366 |

(1999) earthquake and (vi) Nishi- Akashi component of Kobe (1995) earthquake. For excitation of longitudinal direction of the bridge, EW component of time history is used and for excitation of transverse direction, NS component of time history is used. The peak ground accelerations and peak velocities of selected earthquake ground motions are shown in Table 1. Fig. 3 shows the displacement and acceleration response spectra in the transverse and longitudinal directions. The ground motions with full-intensity are assumed to act uniformly at all the supports along the longitudinal and transverse directions of the bridge. The fundamental time period of the uncontrolled bridge is 0.813 sec. At each junction of deck-end and abutment, eight variable dampers are placed, four each along the longitudinal and transverse directions. The configuration of sixteen dampers is adopted to achieve effective energy dissipation in both directions.

To facilitate direct comparison and to evaluate the capabilities of various protective devices and algorithms, a set of 21 evaluation criteria is developed. The criteria are peak base shear force ($J_1$), peak overturning moment ($J_2$), peak displacement at midspan ($J_3$), peak acceleration at midspan ($J_4$), peak deformation of bearings ($J_5$), peak curvature at bent column ($J_6$), peak dissipated energy of curvature at bent column ($J_7$), the number of plastic connections ($J_8$), normed base shear force ($J_9$), normed overturning moment ($J_{10}$), normed displacement at the midspan ($J_{11}$), normed acceleration at midspan ($J_{12}$), normed deformation of bearings ($J_{13}$), normed curvature at bent column ($J_{14}$), peak control force ($J_{15}$), peak stroke of the control devices ($J_{16}$), peak instantaneous power ($J_{17}$), peak total power ($J_{18}$), number of control devices ($J_{19}$), number of sensors ($J_{20}$) and dimension of the discrete state vector i.e., the order of the observer ($J_{21}$). Table 2 presents definition of the evaluation criteria. The evaluation criteria $J_1$ to $J_8$ are defined to measure the reduction in peak response quantities of the benchmark highway bridge; $J_9$ to $J_{14}$ are based on the norm responses and $J_{15}$ to $J_{21}$ are related to the controller. The normed value of the response, denoted $\|\bullet\|$ is defined as $\|\bullet\| = \sqrt{\frac{1}{t_f}\int_0^{t_f}(\bullet)^2 dt}$, where $t_f$ is the time required for the response to attenuate. The present study considers evaluation criteria $J_1$ to $J_{16}$. The evaluation criteria $J_{17}$ and $J_{18}$ are related to the power of the device and are not significant in this study as the power required by the variable dampers is very low. The number of control devices, $J_{19}$ is 16. Since the variable dampers use velocity measurements $J_{20}$ and $J_{21}$, related to control resources and sensors are not discussed in the numerical results. In order to access the performance of variable dampers, the seismic response of the bridge with the friction force scheme and two-step friction force scheme is compared with the corresponding uncontrolled (with LRBs) response and the sample passive, semi-active and active controllers. The response quantities for sample passive, semi-active and active controllers are from Tan and Agrawal (2009). The evaluation

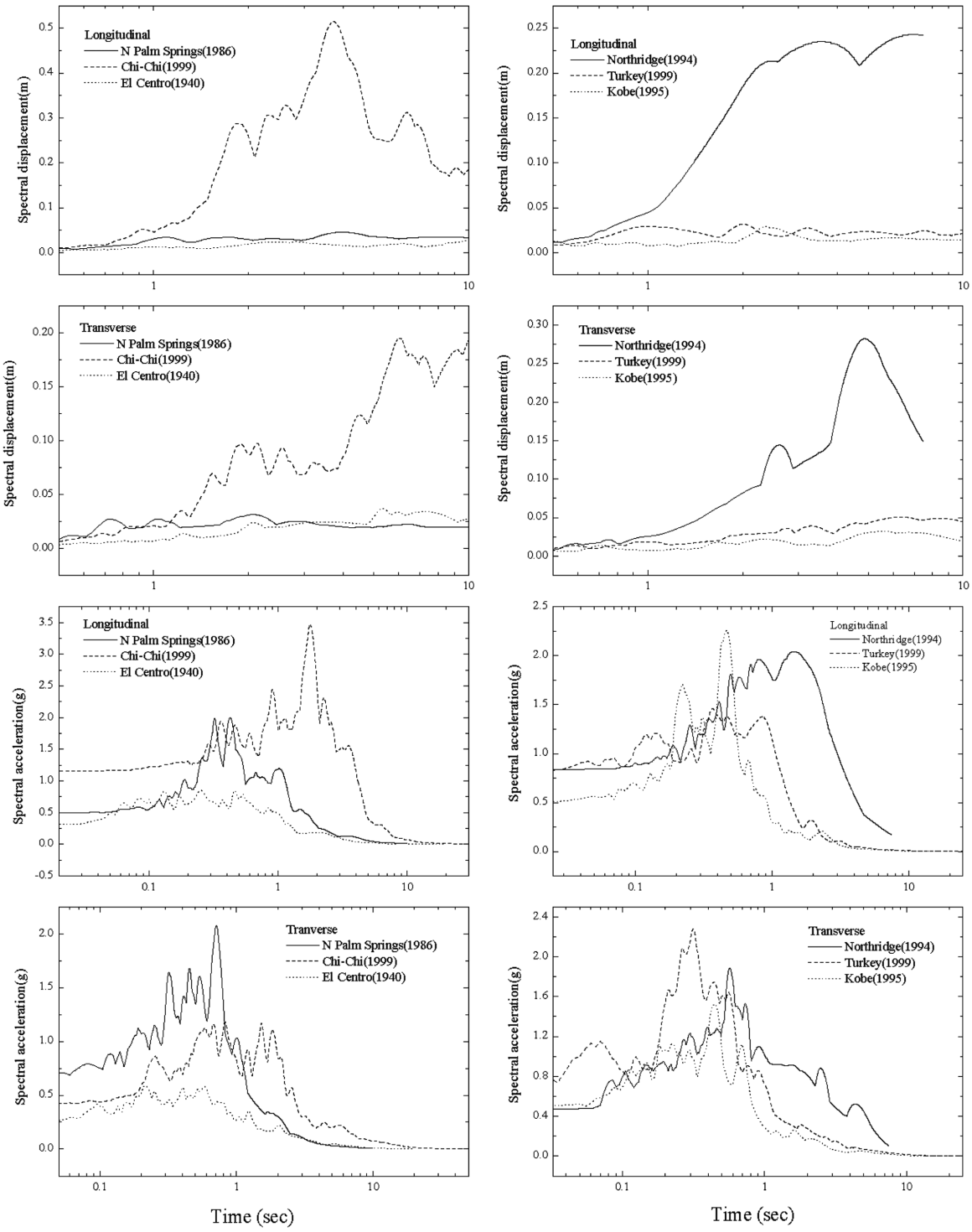


Fig. 3 Displacement and acceleration response spectra for the six earthquake ground motions in the longitudinal ($y$) and transverse ($x$) directions

Table 2 Definition of evaluation criteria

| Peak Responses | Normed Responses | Control Strategy |
|---|---|---|
| Peak Base Shear<br>$J_1 = \max\left\{\frac{\max_{i,t}\lvert F_{bi}(t)\rvert}{F_{0b}^{\max}}\right\}$ | Base Shear<br>$J_9 = \max\left\{\frac{\max_{t}\lVert F_{bi}(t)\rVert}{\lVert F_{0b}^{\max}\rVert}\right\}$ | Peak force<br>$J_{15} = \max\left\{\max_{l,t}\left(\frac{f_l(t)}{W}\right)\right\}$ |
| Peak Overturning Moment<br>$J_2 = \max\left\{\frac{\max_{i,t}\lvert M_{bi}(t)\rvert}{M_{0b}^{\max}}\right\}$ | Overturning Moment<br>$J_{10} = \max\left\{\frac{\max_{t,i}\lVert M_{bi}(t)\rVert}{\lVert M_{0bi}^{\max}\rVert}\right\}$ | Device Stroke<br>$J_{16} = \max\left\{\max_{l,t}\left(\frac{d_l(t)}{x_{0m}^{\max}}\right)\right\}$ |
| Displacement at Midspan<br>$J_3 = \max\left\{\max_{i,t}\left\lvert\frac{y_{mi}(t)}{y_{0m}^{\max}}\right\rvert\right\}$ | Displacement at Midspan<br>$J_{11} = \max\left\{\max_{i}\frac{\lVert y_{mi}(t)\rVert}{\lVert y_{0m}^{\max}\rVert}\right\}$ | Peak power<br>$J_{17} = \max\frac{\max_{t}[\sum_{l} P_l(t)]}{\dot{x}_{0m}^{\max} W}$ |
| Acceleration at Midspan<br>$J_4 = \max\left\{\max_{i,t}\left\lvert\frac{\ddot{y}_{mi}(t)}{\ddot{y}_{0m}^{\max}}\right\rvert\right\}$ | Acceleration at Midspan<br>$J_{12} = \max\left\{\max_{i}\left\lVert\frac{\ddot{y}_{mi}(t)}{\ddot{y}_{0m}^{\max}}\right\rVert\right\}$ | Total Power<br>$J_{18} = \max\left\{\frac{\sum_{l}\int_{0}^{t_f} P_l(t)dt}{x_{0m}^{\max} W}\right\}$ |
| Bearing Deformation<br>$J_5 = \max\left\{\max_{i,t}\left\lvert\frac{y_{bi}(t)}{y_{0b}^{\max}}\right\rvert\right\}$ | Displacement at Abutment<br>$J_{13} = \max\left\{\max_{i}\left\lVert\frac{y_{bi}(t)}{y_{0b}^{\max}}\right\rVert\right\}$ | Control devices<br>$J_{19}$ = number of control devices |
| Ductility<br>$J_6 = \max\left\{\max_{j,t}\frac{\Phi_j(t)}{\Phi^{\max}}\right\}$ | Ductility<br>$J_{14} = \max\left\{\max_{j,t}\left\lVert\frac{\Phi_j(t)}{\Phi^{\max}}\right\rVert\right\}$ | Sensors<br>$J_{20}$ = number of required sensors |
| Dissipated Energy<br>$J_7 = \max\left\{\frac{\max_{j,t}\int dE_j}{E^{\max}}\right\}$ | Plastic Connections<br>$J_8 = \max\left\{\frac{N_d^c}{N_d}\right\}$ | Computational resource<br>$J_{21} = \dim(x_k^c)$ |

criteria are based on the investigated optimum parameters of the control devices. Evaluation criteria are compared for all earthquakes; however, the time-history response is plotted for the Chi-Chi (1999) earthquake, in the longitudinal and transverse direction of the bridge. The main response quantities of interest are the base shear in piers ($J_1$), mid-span deck displacement ($J_3$), bearing (abutment) deformation ($J_5$), and their corresponding normed values ($J_9$, $J_{11}$ and $J_{13}$ respectively). The base shear in the piers indicates the forces exerted in the bridge due to earthquake ground motion. On the other hand, the relative displacement of the control devices is crucial from the design point of view of the control system.

### *5.1 Parametric study on two-step friction force scheme*

A parametric study is performed to investigate the effect of variation in the friction damping force $F_F$, the step-coefficient $\alpha$ and the transitional velocity $\dot{u}_t$ of the two-step friction force scheme, on

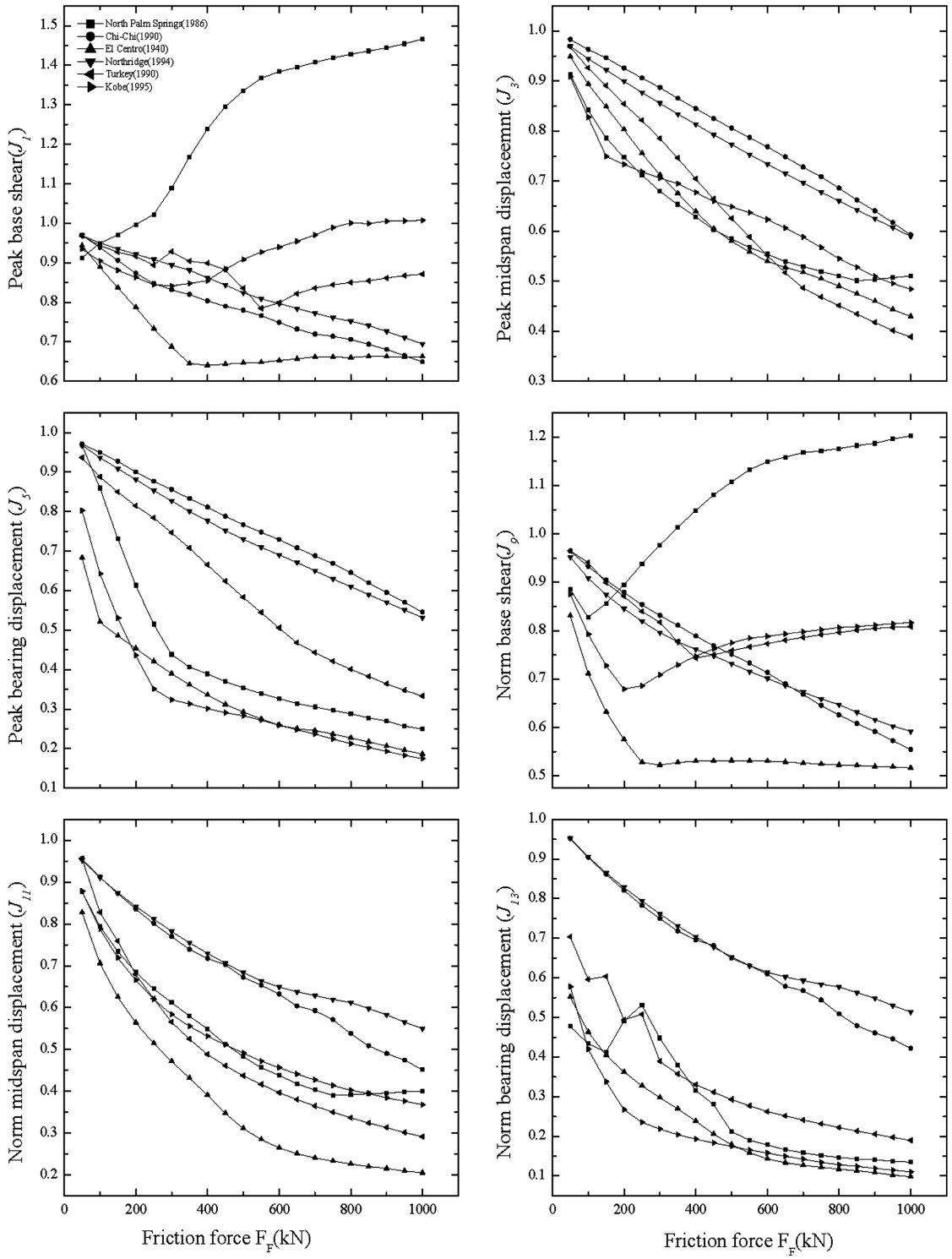


Fig. 4 Variation of $F_F$ for $\alpha = 0.5$ and $\dot{u}_t = 0.2$ m/s for the two-step friction force scheme

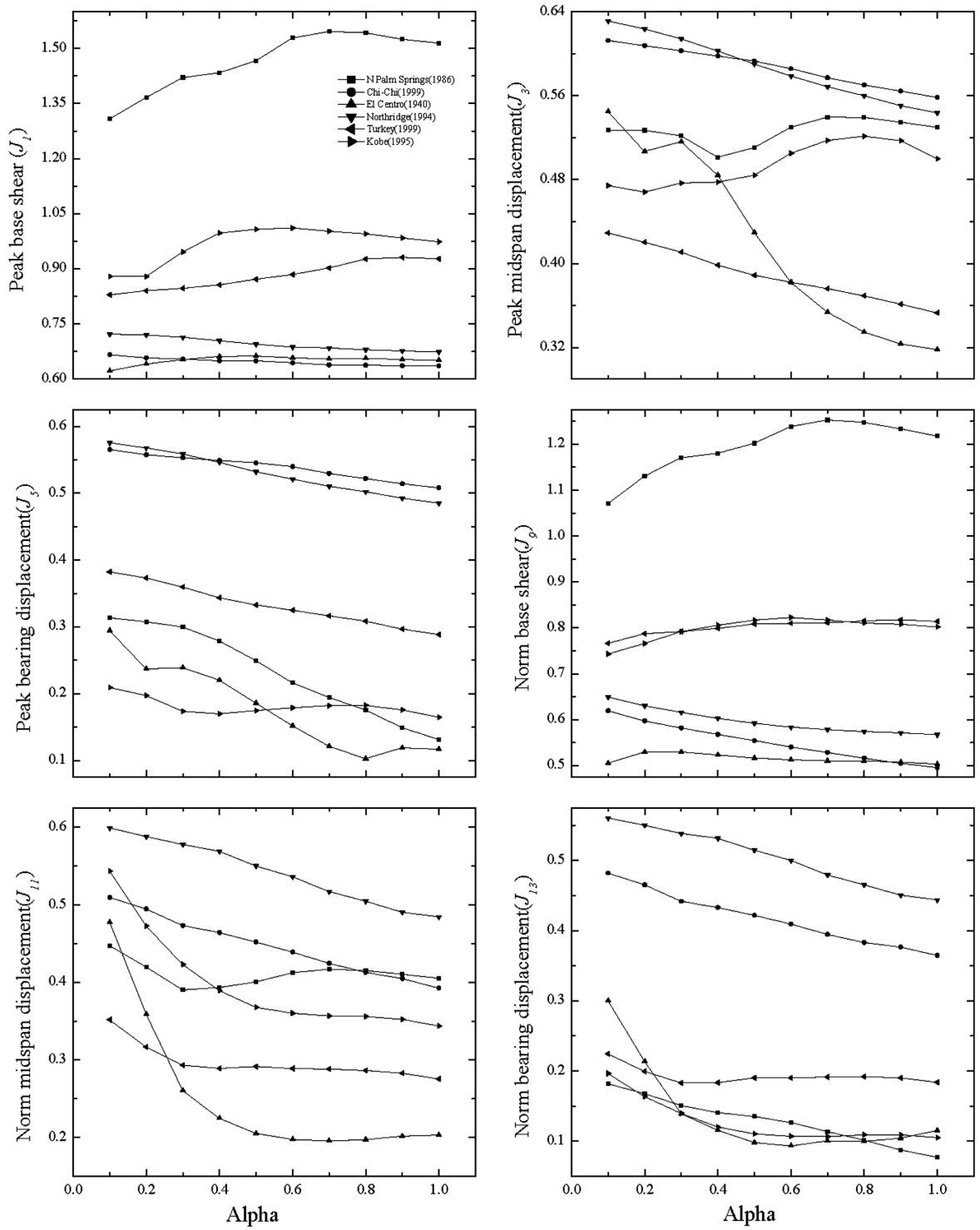


Fig. 5 Variation of $\alpha$ for $F_F$ = 1000 kN and $\dot{u}_t$ = 0.2 m/s for the two-step friction force scheme

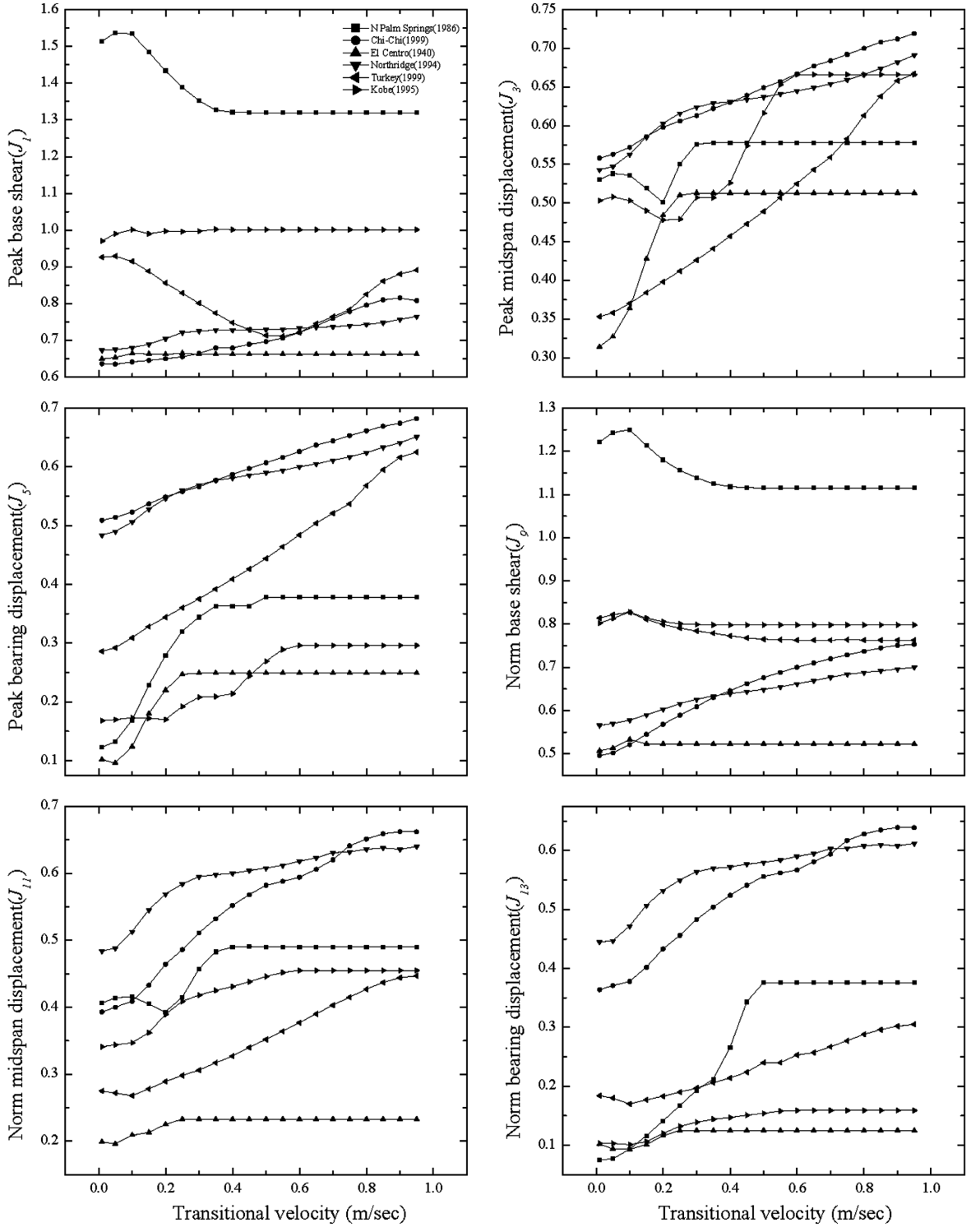


Fig. 6 Variation of $\dot{u}_t$ for $F_F$ = 1000 kN and $\alpha$ = 0.5 for the two-step friction force scheme

the response quantities. Initially, $\alpha$ and $\dot{u}_t$ are assumed as 0.5 and 0.2 m/s, respectively and $F_F$ is varied from 50 to 1000 kN. The results are presented in Fig. 4. It is observed that for Turkey and Kobe earthquakes, the pier base shear reduces with an increase in the damping force up to a certain level and then again increases at a slower rate, giving an optimum value in the range of 200 to 400 kN. For North Palm Springs earthquake, the response continuously increases with increase in damping force of variable dampers, however for Chi-Chi, El Centro and Northridge earthquake, the base shear reduces as the damping force increases. Further, it can be seen from the Fig. 4 that, with increase in the damping force, the displacement response reduces significantly. Hence, for further numerical simulations, the damping force of variable dampers $F_F$ is considered as 1000 kN. Considering 16 control devices, the total damping force provided is about 50% of the weight of the deck. For $\dot{u}_t = 0.2$ m/s, $\alpha$ is varied from 0.1 to 0.9. The results of the study are presented in Fig. 5. The trend of the results indicates that the displacement response reduces gradually with an increase in the coefficient $\alpha$. Further, as depicted from the Fig. 5, the base shear response increases, but at a much slower rate with increase in $\alpha$, for North Palm Springs, Turkey and Kobe earthquake. For Chi-Chi, El Centro and Northridge earthquakes, base shear goes on reducing gradually. Considering base shear and displacement response, a mid-value of $\alpha$ equal to 0.5 is decided for the further study. Thus, the first step of damping force occurs at 500 kN and the second step at 1000 kN. Though displacements continue to decrease further with increasing $\alpha$, the reduction is very marginal beyond $\alpha = 0.5$. Finally, the third parameter, transitional velocity is varied from 0.05 to 0.95 m/s. The results of the study are presented in Fig. 6. Except for North Palm Springs and Turkey earthquake, lower value of $\dot{u}_t$ is favourable for all earthquakes, considering base shear response. For North Palm Springs earthquake, for any value of $\dot{u}_t$, the base shear exceeds the uncontrolled response by 30 to 50%. The displacement response is generally found to increase with $\dot{u}_t$. But, for any value of the transitional velocity, there is substantial reduction in the displacements. For North Palm Springs and Kobe earthquake, the displacements increase at a higher rate beyond $\dot{u}_t = 0.2$ m/s. Also, energy dissipation is found to improve at this velocity giving required shape of the force-displacement loop. Since the optimum values of parameters vary with the earthquake ground motions, the values of parameters are judiciously selected as $F_F = 1000$ kN, $\alpha = 0.5$, $\dot{u}_t = 0.2$ m/s, which yield a maximum reduction in the displacement of the deck and abutment of the bridge, without hampering the significant gain achieved in the base shear response.

Thus, the results of the parametric study performed by varying $F_F$, $\alpha$ and $\dot{u}_t$ suggest that the use of variable dampers as a supplemental damping device is beneficial for reduction in seismic response of the benchmark highway bridge. It is observed that this semi-active device, with simple controlling mechanism of damper force based on the velocity of the device is capable of controlling the displacement response of the deck and bearings at abutments while simultaneously limiting the base shear response of the piers.

### *5.2 Time - history analyses*

The results of time history analyses along the longitudinal and transverse directions are presented in Fig. 7 for the benchmark highway bridge with two-step friction force scheme of variable dampers under the Chi-Chi, 1999 earthquake. The results obtained with LRB isolation system only (uncontrolled response) and with two-step friction scheme of variable dampers are plotted in the same graph for the purpose of comparison. It is observed that there is no increase in the pier base shear response in both directions. In the transverse direction, the response reduces by 11% and by 33% in the

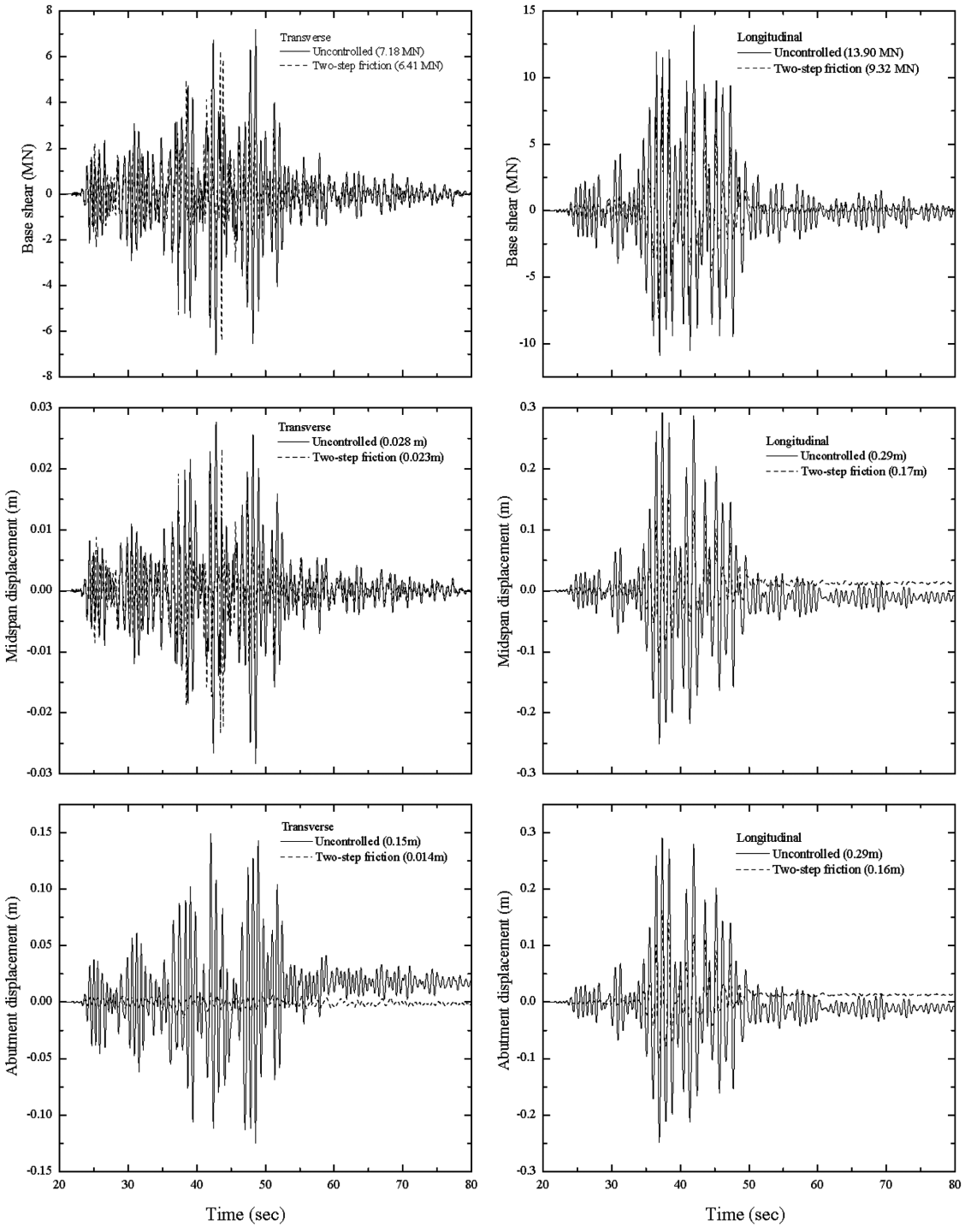


Fig. 7 Time variation of base shear, mid-span displacement and abutment-bearing displacement along the longitudinal and transverse direction of the benchmark highway bridge with variable dampers under Chi-Chi, 1999 earthquake motion

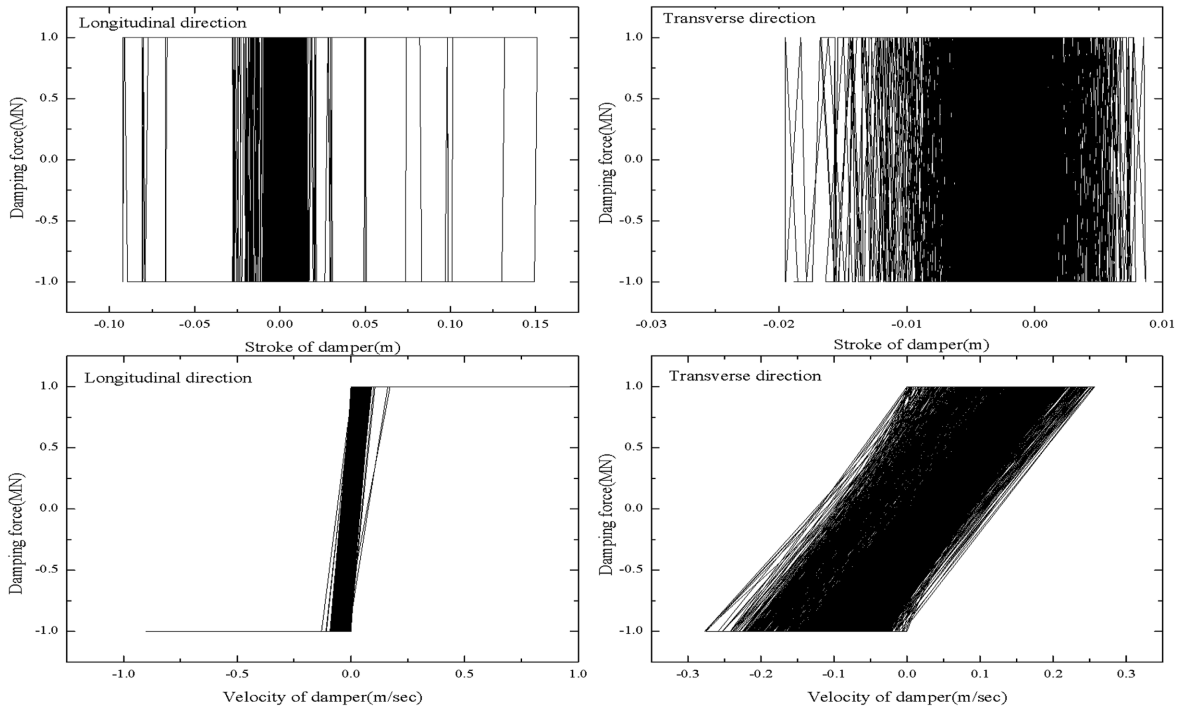


Fig. 8 Force-displacement and force-velocity variation in the longitudinal and transverse direction for friction force scheme of variable dampers

longitudinal direction. It is observed from the time variation plots that the reduction in the displacement response of the bearings at the abutments is remarkable for the bridge with two-step friction scheme of variable dampers. The abutment displacements reduce to only 10% in the transverse direction to 55% in the longitudinal direction. The reduction in the mid-span displacement is marginal in the transverse direction, but substantial in the longitudinal direction.

### *5.3 Force-deformation and force-velocity variation of friction force scheme*

Fig. 8 shows the force-displacement and force-velocity variation in the longitudinal and transverse direction for the friction force scheme of variable dampers. The stroke of damper in the longitudinal direction varies between -0.09 to 0.15 m and in the transverse direction, from -0.02 to 0.009 m. From the plots, it is clear that the dampers oriented along the longitudinal direction of the bridge provide more energy dissipation. The friction force scheme provides a constant damping force for the entire range of the stroke, leading to a rectangular hysteresis loop. Larger enclosed area of the loop indicates that the damper is capable of dissipating substantial amount of energy during the instants of large dynamic responses. The dark area of the loop implies faster fluctuation in direction of the force. For the friction force scheme, the change in velocity of the damper in the longitudinal direction is from -0.9 to 1.16 m/s and in the transverse direction from -0.28 to 0.26 m/s. When velocity of damper is small and changes its sign, the damping forces change suddenly. In the transverse direction, the graphs follow the same pattern as the damping schemes, presented in Fig. 2.

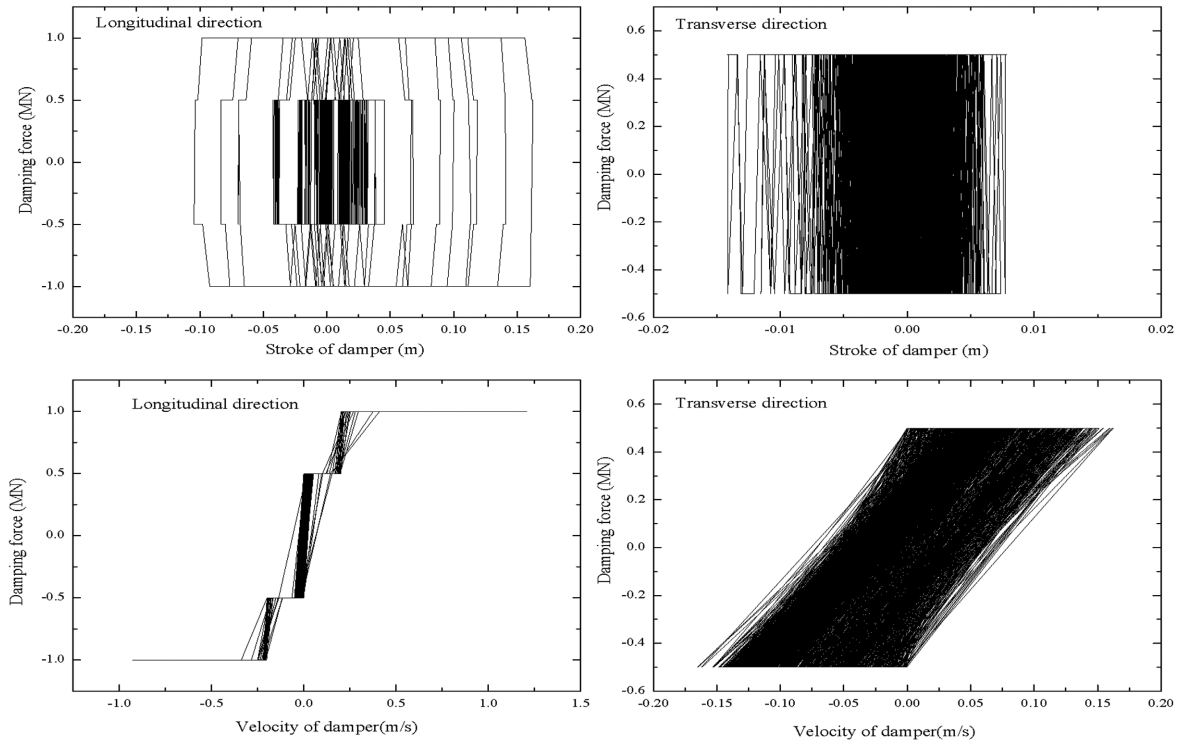


Fig. 9 Force-displacement and force-velocity variation in the longitudinal and transverse direction for two-step friction force scheme of variable dampers

### 5.4 Force-deformation and force-velocity variation of two-step friction force scheme

Fig. 9 shows the force-displacement and force-velocity variation in the longitudinal and transverse direction for the two-step friction force scheme of variable dampers. It is observed that the two-step scheme works well in the longitudinal direction. From the force-velocity plots, a step change of damping force from 500 kN and 1000 kN, at the transitional velocity 0.2 m/s is observed. The displacement loop also shows the change in response at the step. As expected, the graphs follow the same pattern as the damping schemes, presented in Fig. 2.

### 5.5 Evaluation criteria

The evaluation criteria for the sample passive, semi-active, active and the friction and two-step friction schemes of variable dampers are presented in Tables 3-5. In Table 3, evaluation criteria $J_1$ to $J_5$ are compared for all six earthquakes. For Chi-Chi and Northridge earthquake, friction force scheme is the most effective in reducing the peak base shear. For El Centro earthquake, both schemes perform better than the sample semi-active and active control strategies. Peak base moment response is best controlled by the friction force scheme. Except for North Palm Springs earthquake, its performance is much better than all the sample controllers. The performance of both schemes is comparable to each other. For all six earthquakes, the response is substantially improved over the sample controllers.

Table 3 Evaluation criteria $J_1$ to $J_5$ for sample passive, semi-active, active control strategy and friction and two-step friction scheme of variable dampers, for North Palm Springs 1986, Chi-Chi 1999, El Centro 1940, Northridge 1994, Turkey 1999 and Kobe 1995 earthquake

| Response quantity | Control strategy | N Palm Springs | Chi-Chi | El Centro | Northridge | Turkey | Kobe |
|---|---|---|---|---|---|---|---|
| Peak base shear, $J_1$ | P | 1.224 | 0.763 | **0.636** | 0.775 | **0.776** | 0.860 |
| | SA | 0.962 | 0.842 | 0.779 | 0.886 | 0.904 | 0.817 |
| | A | **0.950** | 0.877 | 0.790 | 0.896 | 0.912 | **0.789** |
| | Friction | 1.515 | **0.635** | 0.653 | **0.674** | 0.925 | 0.969 |
| | 2 Step friction | 1.466 | 0.650 | 0.663 | 0.695 | 0.871 | 1.007 |
| Peak base moment, $J_2$ | P | **0.633** | 0.959 | 0.576 | 0.960 | 0.879 | 0.549 |
| | SA | 0.748 | 0.978 | 0.708 | 0.979 | 0.979 | 0.666 |
| | A | 0.770 | 0.966 | 0.742 | 0.978 | 0.978 | 0.704 |
| | Friction | 0.786 | **0.949** | **0.356** | **0.931** | **0.548** | **0.488** |
| | 2 Step friction | 0.759 | 0.950 | 0.392 | 0.943 | 0.568 | 0.507 |
| Peak mid-span displacement, $J_3$ | P | 0.642 | 0.713 | 0.653 | 0.703 | 0.587 | 0.632 |
| | SA | 0.802 | 0.785 | 0.775 | 0.857 | 0.717 | 0.663 |
| | A | 0.823 | 0.799 | 0.779 | 0.867 | 0.746 | 0.704 |
| | Friction | 0.530 | **0.558** | **0.322** | **0.544** | **0.353** | 0.500 |
| | 2 Step friction | **0.510** | 0.593 | 0.430 | 0.590 | 0.389 | **0.484** |
| Peak mid-span acceleration, $J_4$ | P | 1.296 | 0.954 | 0.940 | 0.901 | 0.937 | 1.072 |
| | SA | 0.981 | 0.876 | 0.896 | 0.899 | 0.801 | 0.986 |
| | A | **0.794** | **0.875** | **0.883** | 0.844 | **0.798** | **0.899** |
| | Friction | 1.524 | 0.891 | 0.964 | **0.836** | 1.134 | 1.170 |
| | 2 Step friction | 1.554 | 0.919 | 0.980 | 0.880 | 1.083 | 1.312 |
| Peak bearing deformation, $J_5$ | P | 0.397 | 0.671 | 0.344 | 0.661 | 0.542 | 0.275 |
| | SA | 0.812 | 0.765 | 0.566 | 0.853 | 0.674 | 0.512 |
| | A | 0.937 | 0.803 | 0.643 | 0.883 | 0.714 | 0.586 |
| | Friction | **0.125** | **0.509** | **0.106** | **0.485** | **0.287** | **0.164** |
| | 2 Step friction | 0.250 | 0.546 | 0.186 | 0.532 | 0.333 | 0.175 |

[**Bold** number indicates minimum value]

Friction schemes of variable dampers are not very effective in reducing the mid-span accelerations. This is because the rapid fluctuation of damping force increases the dynamic response of the bridge, causing an increase in the absolute acceleration. Bearing displacement is a quantity of prime interest in the design of isolated bridges because if it exceeds certain limits the bearing may fail resulting into the collapse of the bridge. It is substantially reduced due to friction control. In longitudinal direction, the peak bearing displacement at abutment location with and without variable dampers is found to be 0.16 and 0.29 m, respectively. On the other hand, bearing displacements in the transverse direction are found to decrease from 0.15 to 0.014 m. The performance of the two-step friction scheme is comparable to that of the friction scheme. The analytical investigation indicates that the results are much better compared to the sample control strategies, confirming the effectiveness of variable dampers for displacement response reduction for the benchmark highway bridge. The large displacement responses of the LRB isolators are significantly reduced, with little or no increase in

Table 4 Evaluation criteria $J_6$ to $J_{10}$ for sample passive, semi-active, active control strategy and friction and two-step friction scheme of variable dampers, for North Palm Springs 1986, Chi-Chi 1999, El Centro 1940, Northridge 1994, Turkey 1999 and Kobe 1995 earthquake

| Response quantity | Control strategy | N Palm Springs | Chi-Chi | El Centro | Northridge | Turkey | Kobe |
|---|---|---|---|---|---|---|---|
| Peak ductility, $J_6$ | P | **0.633** | 0.598 | 0.576 | 0.585 | 0.542 | 0.275 |
| | SA | 0.748 | 0.696 | 0.708 | 0.828 | 0.674 | 0.512 |
| | A | 0.770 | 0.743 | 0.742 | 0.852 | 0.714 | 0.586 |
| | Friction | 0.786 | **0.375** | **0.356** | **0.332** | **0.287** | **0.164** |
| | 2 Step friction | 0.759 | 0.449 | 0.392 | 0.402 | 0.333 | 0.175 |
| Peak dissipated energy, $J_7$ | P | **0** | 0.226 | **0** | 0.333 | **0** | **0** |
| | SA | **0** | 0.468 | **0** | 0.567 | 0.236 | **0** |
| | A | **0** | 0.512 | **0** | 0.624 | 0.332 | **0** |
| | Friction | **0** | **0.029** | **0** | **0.091** | **0** | **0** |
| | 2 Step friction | **0** | 0.044 | **0** | 0.146 | **0** | **0** |
| Maximum plastic connections, $J_8$ | P | **0** | 0.667 | **0** | 0.750 | 0 | **0** |
| | SA | **0** | 0.667 | **0** | 1 | 0.333 | **0** |
| | A | **0** | 0.667 | **0** | 1 | 0.333 | **0** |
| | Friction | **0** | **0.333** | **0** | **0.500** | 0 | **0** |
| | 2 Step friction | **0** | 0.500 | **0** | **0.500** | 0 | **0** |
| Norm base shear, $J_9$ | P | 1.031 | 0.747 | 0.518 | 0.709 | **0.738** | 0.746 |
| | SA | 0.779 | 0.846 | 0.597 | 0.829 | 0.840 | **0.691** |
| | A | **0.743** | 0.885 | 0.676 | 0.867 | 0.894 | 0.739 |
| | Friction | 1.218 | **0.496** | **0.504** | **0.567** | 0.814 | 0.803 |
| | 2 Step friction | 1.202 | 0.555 | 0.517 | 0.592 | 0.809 | 0.817 |
| Norm base moment, $J_{10}$ | P | **0.529** | 0.747 | 0.393 | **0.718** | 0.366 | 0.515 |
| | SA | 0.662 | 0.798 | 0.559 | 0.838 | 0.502 | 0.656 |
| | A | 0.696 | 0.834 | 0.643 | 0.878 | 0.532 | 0.713 |
| | Friction | 0.602 | **0.529** | **0.255** | 0.756 | **0.226** | **0.422** |
| | 2 Step friction | 0.594 | 0.596 | 0.261 | 0.721 | 0.236 | 0.430 |

[**Bold** number indicates minimum value]

the pier base shear.

In Table 4, evaluation criteria $J_6$ to $J_{10}$ are compared for all six earthquakes. Minimum number of plastic hinges formed indicates that moment at any section of piers of the bride is less than the fully plastic moment. The friction force scheme works well in reducing the norm base shear. Except for North Palm Springs earthquake, the response reduction is in the range of 20% to 50%. Further, the performance of both the friction schemes is comparable to each other. For norm base moment, friction force scheme is most efficient. It shows improved response over the sample semi-active and active strategies for all earthquakes. Table 5 presents evaluation criteria $J_{11}$ to $J_{14}$ and $J_{16.}$ For norm mid-span displacement, the performance of friction scheme is much superior to all the sample control strategies. Variable dampers are not very effective in reducing the norm mid-span acceleration, except for the near-fault Chi-Chi and Northridge earthquake. For improving the norm bearing displacement, friction force scheme performs very well. Both schemes of variable dampers perform

Table 5 Evaluation criteria $J_{11}$ to $J_{14}$ and $J_{16}$ for sample passive, semi-active, active control strategy and friction and two-step friction scheme of variable dampers, for North Palm Springs 1986, Chi-Chi 1999, El Centro 1940, Northridge 1994, Turkey 1999 and Kobe 1995 earthquake

| Response quantity | Control strategy | N Palm Springs | Chi-Chi | El Centro | Northridge | Turkey | Kobe |
|---|---|---|---|---|---|---|---|
| Norm mid-span displacement, $J_{11}$ | P | 0.557 | 0.645 | 0.410 | 0.650 | 0.442 | 0.544 |
| | SA | 0.683 | 0.753 | 0.580 | 0.777 | 0.573 | 0.675 |
| | A | 0.703 | 0.784 | 0.656 | 0.805 | 0.607 | 0.729 |
| | Friction | 0.405 | **0.392** | **0.204** | **0.485** | **0.274** | **0.343** |
| | 2 Step friction | **0.400** | 0.452 | 0.205 | 0.550 | 0.291 | 0.368 |
| Norm mid-span acceleration, $J_{12}$ | P | 1.017 | 0.765 | 0.743 | 0.777 | 1.008 | 1.059 |
| | SA | 0.789 | 0.807 | 0.690 | 0.818 | 0.809 | 0.837 |
| | A | **0.723** | 0.791 | **0.685** | 0.796 | **0.795** | **0.798** |
| | Friction | 1.222 | **0.625** | 0.741 | **0.736** | 1.144 | 1.179 |
| | 2 Step friction | 1.195 | 0.648 | 0.760 | 0.738 | 1.128 | 1.199 |
| Norm bearing deformation, $J_{13}$ | P | 0.251 | 0.616 | 0.248 | 0.616 | 0.291 | 0.196 |
| | SA | 0.454 | 0.746 | 0.393 | 0.774 | 0.405 | 0.355 |
| | A | 0.483 | 0.784 | 0.484 | 0.821 | 0.521 | 0.472 |
| | Friction | **0.079** | **0.364** | 0.111 | **0.445** | **0.181** | **0.105** |
| | 2 Step friction | 0.135 | 0.422 | **0.098** | 0.515 | 0.190 | 0.110 |
| Norm ductility, $J_{14}$ | P | **0.529** | 0.657 | 0.393 | 0.994 | 0.035 | 0.515 |
| | SA | 0.662 | 0.693 | 0.559 | **0.771** | 0.220 | 0.656 |
| | A | 0.696 | 0.648 | 0.643 | 0.827 | 0.239 | 0.713 |
| | Friction | 0.602 | **0.620** | **0.255** | 1.223 | **0.022** | **0.422** |
| | 2 Step friction | 0.594 | 0.708 | 0.261 | 1.205 | 0.023 | 0.430 |
| Maximum device stroke, $J_{16}$ | P | 0.382 | 0.642 | 0.317 | 0.602 | 0.537 | 0.271 |
| | SA | 0.782 | 0.732 | 0.521 | 0.777 | 0.669 | 0.505 |
| | A | 0.902 | 0.769 | 0.592 | 0.804 | 0.708 | 0.578 |
| | Friction | **0.120** | **0.487** | **0.098** | **0.442** | **0.284** | **0.162** |
| | 2 Step friction | 0.240 | 0.522 | 0.171 | 0.485 | 0.330 | 0.172 |

[**Bold** number indicates minimum value]

efficiently than all the sample control strategies with norm bearing displacement reduction in the range of 55% to 90%. The amount of displacement is quite small to have any possible impact of the deck with the abutments in longitudinal direction or with the bent piers in the transverse direction. Table 6 compares the numerical values of critical response quantities, namely base shear, base moment, midspan displacement, midspan acceleration and bearing displacement for the uncontrolled (with LRBs) and controlled case with variable dampers.

The results of the investigation demonstrate that variable dampers with friction force schemes are capable of controlling the peak displacement response of the bridge, isolated with LRBs, and thus reducing the length of expansion joints. Further more, except for North Palm Springs earthquake, the peak base shear is also controlled effectively. In general, the evaluation criteria are smaller than one, indicating that the friction force schemes of variable dampers are capable of reducing the response of the benchmark highway bridge for a wide variety of earthquake records. Hence, the use

Table 6 Comparison of numerical values of critical response quantities

| | N.Palm Springs | Chi-Chi | El Centro | Northridge | Turkey | Kobe |
|---|---|---|---|---|---|---|
| Control strategy | | | Base shear (N) | | | |
| Uncontrolled | 5.90E+06 | 1.87E+07 | 5.81E+06 | 1.94E+07 | 1.27E+07 | 6.90E+06 |
| Friction force | **8.94E+06** | 1.19E+07 | 3.79E+06 | 1.31E+07 | 1.18E+07 | 6.69E+06 |
| Two-step friction force | **8.64E+06** | 1.21E+07 | 3.85E+06 | 1.35E+07 | 1.11E+07 | **6.95E+06** |
| | | | Base moment (Nm) | | | |
| Uncontrolled | 2.76E+07 | 5.53E+07 | 2.58E+07 | 5.61E+07 | 5.26E+07 | 3.33E+07 |
| Friction force | 2.17E+07 | 5.25E+07 | 9.20E+06 | 5.22E+07 | 2.88E+07 | 1.62E+07 |
| Two-step friction force | 2.10E+07 | 5.26E+07 | 1.01E+07 | 5.29E+07 | 2.98E+07 | 1.69E+07 |
| | | | Midspan displacement(m) | | | |
| Uncontrolled | 0.06196 | 0.292 | 0.0568 | 0.31 | 0.182 | 0.0752 |
| Friction force | 0.03285 | 0.163 | 0.0183 | 0.17 | 0.064 | 0.0377 |
| Two-step friction force | 0.03163 | 0.173 | 0.0244 | 0.18 | 0.071 | 0.0364 |
| | | | Midspan acceleration(m/sec$^2$) | | | |
| Uncontrolled | 5.715 | 13.079 | 3.777 | 14.412 | 9.847 | 5.43 |
| Friction force | **8.17** | 11.7 | 3.642 | 12.055 | **11.168** | **6.354** |
| Two-step friction force | **8.88** | 12 | 3.703 | 12.69 | **10.666** | **7.123** |
| | | | Bearing displacement (m) | | | |
| Uncontrolled | 0.0937 | 0.299 | 0.101 | 0.316 | 0.19 | 0.16 |
| Friction force | 0.0117 | 0.152 | 0.011 | 0.153 | 0.055 | 0.026 |
| Two-step friction force | 0.0234 | 0.163 | 0.019 | 0.168 | 0.063 | 0.028 |

[**Bold** number indicates that the response is greater than the uncontrolled response]

of variable dampers as supplemental damping device largely solves the problem of superstructure displacement of an isolated benchmark highway bridge, along with controlling the seismically induced forces in the bridge.

## 6. Conclusions

The efficacy of variable dampers in protecting the benchmark highway bridge subjected to strong earthquake ground motions has been investigated. The variable dampers consist of MR dampers with pre-set velocity-dependent schemes of damping force. The range of velocity acts a controller to the restoring damping forces. The seismic response of a simplified model of the 91/5 highway bridge at Southern California is studied under two horizontal components of six real earthquake ground motions. The seismic responses of the bridge with friction force and two-step friction force scheme have been evaluated using standard numerical technique and the developed SIMULINK models. The comparison of seismic response of the bridge controlled with variable dampers and the sample controllers is made, in order to verify the effectiveness of the variable dampers. From the dynamic analytical investigation of the bridge, with variable dampers, following conclusions are drawn:

1. The supplemental damping in the benchmark highway bridge using variable dampers helps to reduce the displacement response and the base shear response substantially. However, the acceleration

response of the deck increases marginally.

2. The semi-active variable dampers control the earthquake response of the isolated bridge significantly. Specifically, a variable damper of 1000 kN capacity with step coefficient $\alpha$ equal 0.5 and transitional velocity equal to 0.2 m/s is found to be more efficient in controlling the displacement response of the isolated bridge.

3. There exists an optimum amount of damping force provided by variable dampers for controlling the pier base shear response. Optimum value equal to 1000 kN is found for all earthquakes, except for North Palm Springs, 1986 earthquake. However, for the displacement response, no such optimum value is found, as the mid-span displacement and the bearing displacement reduce with an increase in damping force of the variable dampers.

4. With variable dampers as controllers, a maximum reduction in the mid-span displacement response of the isolated bridge by up to about 65% and in the bearing displacements up to about 90%, can be achieved.

5. There is very little or no increase in the pier base shear response of the bridge with variable dampers, compared to that of the isolation system alone and the response by the sample controllers, except for North Palm Springs earthquake. This is because the optimum damping force for this earthquake is much smaller than 1000 kN.

6. The friction force scheme of variable dampers is found to be more effective in controlling the peak displacement response of the deck and abutment bearings while simultaneously limiting the peak pier base shear response. Average reduction in the peak bearing displacement is three times more as compared with the sample active controllers.

## References

Agrawal, A.K., Tan, P., Nagarajaiah, S. and Zhang, J. (2009), "Benchmark structural control problem for a seismically excited highway bridge, part I: problem definition", *Struct. Control Health Monit*., **16**(5), 509-529.

Ali, S.F. and Ramaswamy, A. (2006), "Benchmark control problem for highway bridge based on FLC", *Proceedings of the ASCE Structures Congress 2006*, St. Louis, MO, USA, May.

Choi, K.M., Jung, H.J., Cho, S.W. and Lee, I.W. (2006), "Application of smart passive damping system using MR damper to highway bridge benchmark problem", *Proceedings of the 8th international conference on Motion and Vibration control (MOVIC 2006)*, Daejeon, Korea, August.

Kawashima, K. and Unjoh, S. (1994), "Seismic response control of bridges by variable dampers", *J. Struct. Eng.-ASCE*, **120**(9), 2583-2601.

Kunde, M.C. and Jangid, R.S. (2003), "Seismic behaviour of isolated bridges: A state-of-the-art review", *Electron. J. Struct. Eng*., **3**, 140-170.

Reigles, D.G. and Symans, M.D. (2006), "Response modification of highway bridge benchmark structure using supervisory fuzzy control of smart seismic isolation system", *Proceedings of the ASCE Structures Congress 2006*, St. Louis, MO, USA, May.

Ruangrassamee, A. and Kawashima, K. (2001), "Experimental study on semi-active control of bridges with use of magnetorheological damper", *J. Struct. Eng.-JSCE*, **47A**(2), 639-650.

Ruangrassamee, A. and Kawashima, K. (2002), "Seismic response control of a benchmark cable-stayed bridge by variable dampers", *Proceedings of the American Control Conference 2002*, Anchorage, AK, USA, May.

Ruangrassamee, A. and Kawashima, K. (2003), "Control of nonlinear bridge response with pounding effect by variable dampers", *Eng. Struct*., **25**(5), 593-606.

Ruangrassamee, A. and Kawashima, K. (2006), "Seismic response control of a cable- stayed bridge by variable dampers", *J. Earthq. Eng*., **10**(1), 153-165.

Ruangrassamee, A., Nakamura, G. and Kawashima, K. (2004), "A model test and analysis on seismic response

control of bridges by MR dampers", *Proceedings of the 13th World Conference on Earthquake Engineering*, Vancouver, BC, Canada, August.
Spencer, Jr., B.F., Dyke, S.J., Sain, M.K. and Carlson, J.D. (1997), "Phenomenological model of a magnetorheological damper", *J. Eng. Mech.-ASCE*, **123**(3), 230-238.
Tan, P. and Agrawal, A.K. (2009), "Benchmark structural control problem for a seismically excited highway bridge-Part II: Phase I Sample control designs", *Struct. Control Health Monit*., **16**(5), 530-548.
Zhang, J. and Makris, N. (2002), "Seismic response analysis of highway overcrossings including soil-structure interaction", *Earthq. Eng. Struct. D*., **31**(11), 1967-1991.

*CC*